minerals

MDPI

Article

Correlation of Flotation Recoveries and Bubble–Particle Attachment Time for Dodecyl Ammonium Hydrochloride/Frother/Quartz Flotation System

Khandjamts Batjargal [1], Onur Güven [2], Orhan Ozdemir [3,*], Feridun Boylu [3], Yusuf Enes Pural [3] and Mehmet Sabri Çelik [3,*]

[1] Department of Mining Engineering, Faculty of Engineering, Istanbul University Cerrahpaşa, 34500 Istanbul, Turkey; khandjants@gmail.com
[2] Department of Mining Engineering, Faculty of Engineering, Adana Alparslan Turkes Science and Technology University, 01250 Adana, Turkey; oguven@atu.edu.tr
[3] Department of Mineral Processing Engineering, Faculty of Mines, Istanbul Technical University, 34469 Istanbul, Turkey; boylu@itu.edu.tr (F.B.); pural@itu.edu.tr (Y.E.P.)
* Correspondence: orhanozdemir@itu.edu.tr (O.O.); mcelik@itu.edu.tr (M.S.Ç.)

Abstract: Recent studies in the flotation of fine particles have necessitated new techniques and analyses for developing various strategies. Particularly, the improvements in flotation chemistry including the selection of the type of frother, collector, and other reagents have become very significant. In this study, the effect of different commercial polypropylene glycol frothers (PPG200, 400, and 600) in the presence of dodecylammonium hydrochloride (DAH) was investigated for their contribution to flotation recoveries and bubble–particle attachment time values of fine quartz minerals. Zeta potential measurements with DAH were also carried out as a function of pH and reagent concentration to justify the effect of collector usage alone on the charge of particles. A linear increase in flotation recoveries against collector concentration, e.g., 7.4% recovery at 1×10^{-5} mol/L DAH and 65.4% recovery at 1×10^{-3} mol/L DAH, was obtained. In this context, the contribution of frothers was particularly important in that a recovery of 15.91% in the absence of the frother and a modest increase to 19.70% was obtained upon the addition of PPG600 at its critical coalescence concentration (CCC) of 3 ppm. Finally, a strong correlation was found between the bubble–particle attachment time and flotation recovery as a function of collector concentration (lowest attachment time vs. highest flotation recovery). The latter correlation is very promising because bubble attachment time leads to various micro-mechanisms in flotation including bubble film thinning, bubble rupture, and induction time, and consequently, frother efficiency in the presence and absence of a collector. As a result, the experimental findings were gathered to achieve a consistent base for further fundamental studies on the application of the synergistic effect of frothers and collectors in the flotation of fine particles.

Keywords: flotation; frother; fine particles; attachment time; zeta potential; quartz; dodecyl ammonium hydrochloride

Citation: Batjargal, K.; Güven, O.; Ozdemir, O.; Boylu, F.; Pural, Y.E.; Çelik, M.S. Correlation of Flotation Recoveries and Bubble–Particle Attachment Time for Dodecyl Ammonium Hydrochloride/Frother/Quartz Flotation System. *Minerals* **2023**, *13*, 1305. https://doi.org/10.3390/min13101305

Academic Editors: William Skinner and Longhua Xu

Received: 3 September 2023
Revised: 2 October 2023
Accepted: 7 October 2023
Published: 9 October 2023

1. Introduction

Flotation is a physico-chemical process based on differences in the surface properties of minerals in which hydrophobic (water-repellent) particles are separated from hydrophilic (water-wetted) particles by bubbles and used in many industries, from metallurgical to chemical [1]. The enrichment of minerals with the flotation method depends on selectively making mineral surfaces hydrophobic by adjusting the pH of the medium and introducing the appropriate size of air bubbles [2–5]. If minerals do not possess surface properties akin to the attachment air bubbles, chemicals called collectors are added to make the mineral hydrophobic [6,7]. Additionally, the efficiency of flotation is strongly related to the collecting ability of air bubbles, and their behavior is generally controlled with the use of chemicals

called frothers, which reduce air/liquid interfacial tension [8]. Moreover, particles and bubbles collide, whereby the bubble and the particle approach each other closely, and attachment can occur [9,10] Therefore, bubble–particle attachment is a critical mechanism for successful flotation in terms of colloid and surface chemistry for both particles and air bubbles [11]. Additionally, the type and amount of frothers, collectors, or both are considered as important parameters to achieve a successful flotation separation [12–15].

In recent years, many investigations have been carried out for adjusting flotation conditions such as reagent types [16] and particle-based properties [17–20] to selectively optimize flotation recoveries. Laboratory flotation experiments utilize methods like bubble–particle attachment time [21,22] and zeta potential measurements [22–25] to support the selection of most critical flotation parameters such as pH, reagent type, and concentration, which otherwise may lead to significant losses in the flotation of valuable minerals. At that point, a complementary representation of these aforementioned values will be a good guide for showing the effects of different parameters like frother type, collector type, etc. to optimize the flotation conditions of a target mineral.

In this context, Ahmad and Jameson [2] reported that upon decreasing the bubble size from 655 μm to 75 μm during the flotation of quartz and zircon particles under 50 μm, the flotation rate constant increased up to a hundred-fold. Thus, the flotation results of their study showed the importance of bubble size, which in turn was affected by the frother type and concentration. Another paper reported by Yoon and Luttrell [3] also showed the same trend for the effect of bubble size during the flotation of very hydrophobic coal particles. Their results clearly showed that the flotation recovery values increased in accordance with the decreasing trend in the bubble size. However, they also showed that although a similar trend on flotation recoveries was obtained with decreasing bubble size, relatively lower flotation rate constants were obtained with run-off mine coals; this was attributed to their hydrophobicity degree, which in turn indicated the contribution of the collector usage to adjust the optimum flotation conditions. In another study by Fan et al. [10], possible attachment mechanisms between solid particles and air bubbles with the same sign of zeta potential were investigated. It was found that the attachment of naturally hydrophilic quartz to the air bubble could be obtained upon increasing pH in surfactant-free deionized water. The researchers attributed these findings to the possible hydrogen bond formation at relatively high pH. These studies clearly revealed that bubble and particle charges under the same conditions would be effective parameters during flotation tests. Batjargal et al. [14] recently studied the effect of the mixture of a collector and different frothers on the critical coalescence concentration (CCC) and bubble size distribution. The use of a collector in the system decreased the CCC concentrations of the frothers and produced a wider bubble size distribution, which contributed to better flotation recoveries.

Thus, considering these findings and others in the literature on the effect of parameters such as bubble–particle attachment rate [22,26] or micro-flotation behavior of particles as a function of frother, collector, or their mixtures [27], to our knowledge, only a few of them presented the results of bubble–particle attachment time along with micro-flotation experiments in the presence of frother–collector mixtures. Considering the lack of knowledge in the literature, this study aimed to suggest a relation between bubble–particle attachment time and the corresponding micro-flotation recoveries as a function of collector concentration, and to analyze the effect of the frother type on the flotation recoveries under different collector concentrations.

2. Materials and Methods

2.1. Materials

The quartz sample used in this study was provided by ESAN Mining Company, Istanbul, Turkey. The chemical and mineralogical properties of the sample were analyzed by wet chemical analysis and X-ray diffraction (XRD) methods (D8 advance; Bruker AXS X-ray Diffractometer, Madison, WI, USA). The results of these analyses are shown in Table 1 and Figure 1, respectively. It is worth noting that before experimental studies, the

sample was additionally subjected to a low-intensity wet magnetic separator (WHIMS 3X4L, Carpco Inc., Jacksonville, FL, USA) to eliminate the effect of any kind of possible contamination. The XRD patterns and chemical analyses of the sample shown in Figure 1 and Table 1 indicated that the sample was rather pure enough to carry out fundamental studies such as the contribution of different frothers to the bubble–particle attachment and micro-flotation experiments.

Table 1. Chemical analyses of the sample.

Compound	% by wt.
SiO_2	98.970
Al_2O_3	0.632
Fe_2O_3	0.095
TiO_2	0.095
MgO	0.096
CaO	0.035
Na_2O	0.034
K_2O	0.043

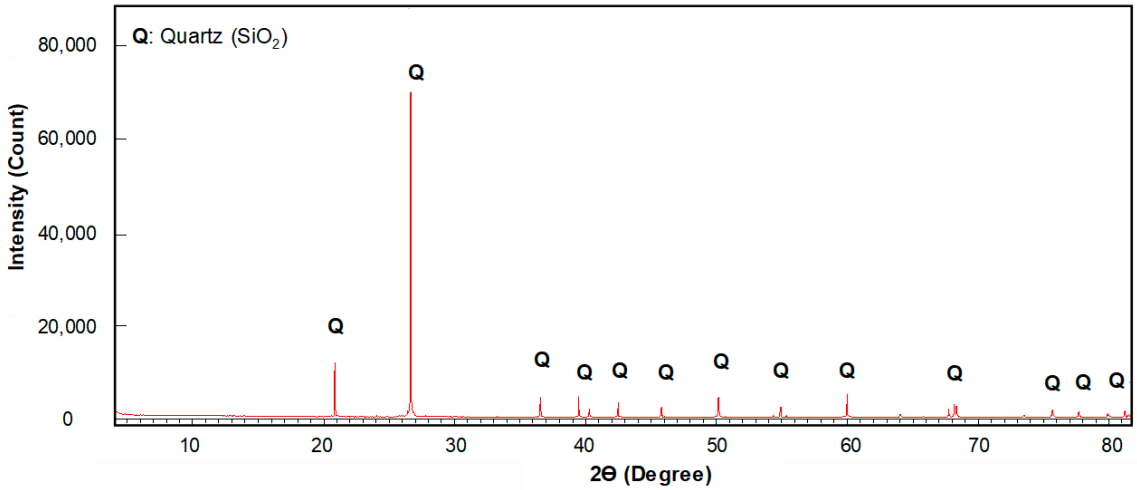

Figure 1. XRD analysis of the sample.

The effect of frother type on flotation recoveries was investigated using commercial frothers, namely polypropylene glycols (PPG200, 400, and 600) obtained from BASF company (Ludwigshafen, Germany), and dodecylamine hydrochloride (DAH, CH_3 $(CH_2)11NH_2$·HCl with 97% purity, Alfa Aesar Company, Ward Hill, MA, USA) was used as a collector for the micro-flotation experiments and zeta potential measurements. Although different cationic collectors with different chain lengths like cetyltrimethylammonium bromide (CTAB), ether or ester amines, or quaternary ammonium salts can be used to float quartz particles. In this study, DAH was selected based on its better performance at low molarities compared to other collectors. The physical and chemical properties of the frothers were given in our previous study in detail [28]. All glassware was rinsed with ethylene alcohol (99% purity, MERCK, Kenilworth, NJ, USA) and washed with pure water, followed by steam cleaning and drying in a clean oven. All the experiments and measurements were conducted at a constant room temperature: 23 ± 1 °C. Hydrochloric acid (HCl, Merck, Germany) and sodium hydroxide (NaOH, Merck, Germany) were used to adjust the pH values of the particles (between pH 1 to 11) during the zeta potential measurements.

2.2. Methods

2.2.1. Sample Preparation

The sample was first crushed by a jaw crusher (BA Crushing Company, Adana, Turkey) to produce particles within −2 + 1 mm size. Then, the crushed sample was ground for 40 min in a dry ceramic cylindrical ball mill of 5200 cm^3 in volume to prevent possible contamination arising from the wear of the grinding media. The particles obtained under 38 μm were split in the size range of −38 + 20 μm (d80 size of the sample is 27.9 μm) by a controlled settling procedure. In this method, the −38 μm sample was placed in a measuring cylinder of 1 L volume, and particles finer than 20 μm were transferred separately from the top of the suspension (around 900 mL line) to another beaker after 1 min of settling. While the size range of −38 + 20 μm was used for the micro-flotation experiments and bubble–particle attachment measurements, the fraction under 10 μm (d80 size of the sample is 8.49 μm) separated from the suspension was only used for the zeta potential measurements. Herein, the particles within −20 + 10 μm (d80 size of the sample is 17.8 μm) were stored for future experiments. The particle size distributions of the quartz samples were determined by the laser light scattering technique (Malvern Particle Sizer 3000, Malvern Instruments, Malvern, UK).

In the literature, different methods like sieving and image analysis were reported to measure the particle size distribution [29]. In this study, a mixture of these methods was sequentially adapted to obtain the target size. It is worth noting that the control of the material under 20 μm was difficult to show the contribution of different frother types on quartz flotation. In other words, a cationic collector such as DAH also functions as a frother, and the flotation of very fine particles would mask the contribution of frothers. The particles under 20 μm were thus removed before the flotation experiments and bubble–particle attachment measurements.

2.2.2. Zeta Potential Measurements

The state of the electrical double layer affects the specific adsorption of the collectors, and all the ions in the solution can adsorb on the outer layer. Before the bubble–particle attachment and micro-flotation experiments, a series of measurements were conducted to characterize the pH profile and the effect of collector concentration in the presence of quartz particles. These measurements were made by the electrophoretic method using a Brookhaven Zetaplus analyzer (Brookhaven Instrument Ltd., Holtsville, NY, USA). In this method, the particles subjected to electric current move according to the electric charges, and the device used measures the speed of the movement of the particles. The zeta potential is automatically calculated according to the Smoluchowski equation.

In these measurements, first, a sample of 0.25 g of 10 μm quartz particles in a 100 mL beaker was mixed with 50 mL of pure water (0.5% solids ratio) using a magnetic stirrer at 500 rpm for 5 min. Second, the desired pH values were achieved by using 0.1 mol/L HCl for the acidic medium and 0.1 mol/L NaOH for the basic medium. Next, the suspension reached an equilibrium pH after 5 min of mixing. Then, a stable suspension that allows the settling of the coarse particles was found to be 5 min. upon the mixing process. Finally, approximately 3 mL aliquots, which were taken from the upper surface layer of the suspension, were transferred to the zeta potential measurement cell of 4 mL in volume.

During the second measurement, a mixture of 0.25 g of 10 μm quartz sample and 50 mL collector (1×10^{-5} mol/L–1×10^{-3} mol/L) was mixed in a 100 mL beaker with a magnetic stirrer; the pH value was measured and recorded after 5 min of conditioning. For each measurement, the zeta potential was measured 20 times, and the mean value was recorded as the final value. All zeta potential measurements were performed at room temperature of 23 °C. The standard deviation value of the measurements was kept around ±2 mV.

2.2.3. Bubble–Particle Attachment Measurements

Literature survey shows that the bubble–particle attachment process plays an important role in terms of flotation recovery, and critical parameters such as bubble and particle size, collector concentration, etc. [30,31]. The bubble–particle attachment measurements were therefore conducted to understand the bubble and particle interactions as a function of DAH concentration using a bubble–particle attachment timer (BKT-100 model, Bratton Engineering and Technical Associates, LLC, USA). The experimental setup used for the bubble–particle attachment measurements is shown in Figure 2. In this method, a retained bubble formed at the tip of a glass capillary is pushed down through the cell containing the particle bed and the liquid phase, and the bubble tip is kept in contact with the particle bed for a controlled contact time. The bubble is then returned to its original position together with the glass capillary. During these experiments, the bubble and the glass capillary are observed with a digital camera to determine whether the particles are attached to their surface after a controlled contact time. The results from the observations of "attachment" and "no attachment" are recorded to calculate the bubble–particle attachment efficiency at a constant contact time. The bubble–particle attachment time is determined based on 50% of the observations that result in attachment at a specific contact time. Meanwhile, the images of particles attached to the bubbles are also taken using a CCD camera (Hikvision, China) to analyze the bubble–particle interactions in detail.

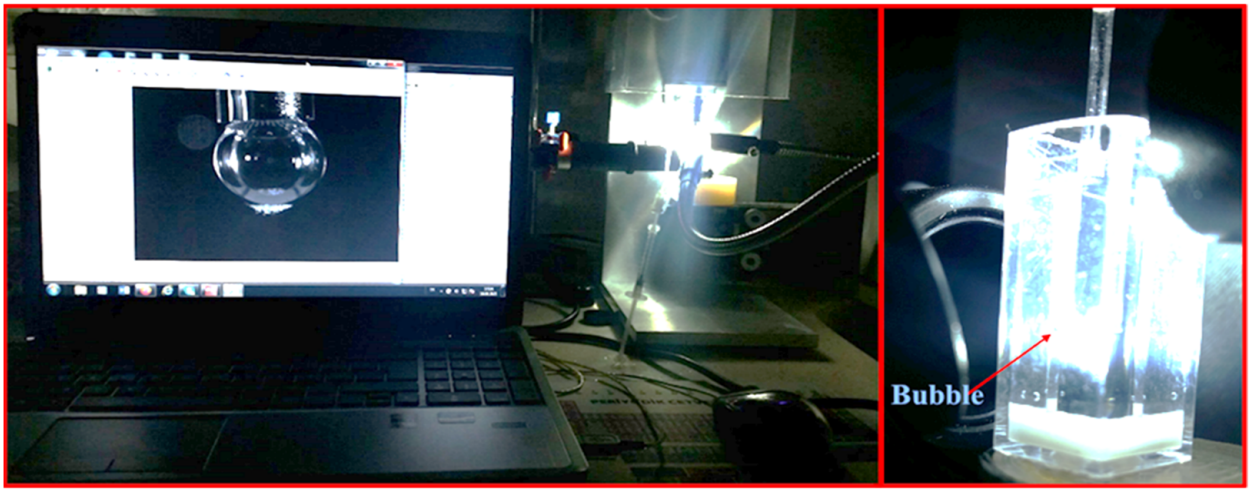

Figure 2. Experimental setup of bubble–particle attachment.

The bubble–particle attachment measurements were carried out with a 0.5 g pure quartz sample and 50 mL collector solution (1% solids by wt.) being conditioned for 10 min to ensure that the collector adsorbed effectively on the mineral surface. After the conditioning process, the suspension was kept for 2 min, and a sufficient amount of sample was taken and placed in the measuring cell. The bed thickness in the cell was approximately 2.5 mm and the cell volume was 4 mL. The bubble–particle attachment measurements were made using 3 different radii of glass capillaries (0.5 mm, 1 mm, and 2 mm). Additionally, it was assumed that the sizes of both the bubble and the capillary tube coincided. Our previous results indicated that the bubble–particle attachment efficiency was proportional to the capillary pressure and the size of the bubble [32]. Therefore, the measurements were carried out with the smallest capillary size of 0.5 mm for the fine quartz particles. A series of measurements was conducted at different concentrations such as 1×10^{-5}, 5×10^{-5}, 1×10^{-4}, 5×10^{-4}, and 1×10^{-3} mol/L DAH at 1, 10, 100, and 1000 ms contact times to determine the effect of collector concentration on attachment time. The bubble–particle attachment experiments were repeated 20 times for each concentration at different spots on the quartz particle surfaces. All measurements were carried out at 23 °C at room temperature.

2.2.4. Micro-Flotation Experiments

The micro-flotation experiments were carried out with −38 + 20 μm quartz particles using a 155 mL micro-flotation column cell (30 mm × 220 mm) with a ceramic frit (pore size of 16 μm). In the experimental studies, 1 g of sample was first conditioned with the reagent solutions (frother and collector) at different concentrations for 5 min in a glass beaker at 250 mL volume and 480 rpm. All the experiments were carried out at natural pH (measured as 6.30 ± 0.10) to eliminate the effect of pH on the flotation recovery. When the conditioning was completed, the suspension was transferred to the flotation cell and the samples were floated for 1 min using N_2 gas at a flow rate of 50 cm^3/min. The float and sink products of the flotation process were dewatered with filter paper and dried at 105 °C in a drying oven. The amount of quartz particles in both the float and sink products was determined by gravimetric analysis. The flotation recovery was calculated based on the weight of the floated concentrate in the feed. It is worth mentioning that all experiments were repeated three times, and the average flotation recovery value was calculated for each experiment.

3. Results and Discussion

3.1. Zeta Potential Measurements

The zeta potential value is particularly important for silicate and oxide minerals, where the adsorption of collectors is dependent on surface charge. Additionally, the zeta potential measurements representing the electrokinetic properties of minerals reveal important information for understanding the flotation mechanism of minerals. For this purpose, the zeta potential measurements for the quartz particles (−10 μm) were performed to determine the electrophoretic mobility of the particles. Figure 3 shows the results for the zeta potential pH profile of the quartz sample in the absence of DAH (Figure 3a), and the zeta potential distribution of the quartz samples as a function of DAH concentration (Figure 3b).

The measurements illustrating the effect of pH on the zeta potential of quartz particles (Figure 3a) indicated that the isoelectric point (iep) value of quartz is 1.8. These results are in line with the previous studies reported in the literature [33]. The surface charge of quartz was positive at acidic pH values lower than pH 1.8 and reached up to 4.63 mV at pH 1.28. Additionally, at basic pH values higher than pH 1.8, the surface charge of quartz was negative, and the surface charge increased up to −78.25 mV at pH 11.16. In addition, the zeta potential of pure quartz was found to be −30.30 mV at the natural pH of 6.30.

Based upon this knowledge, another series of analyses was conducted to determine the effect of collector concentration on the zeta potential values of quartz particles. The results presented in Figure 3b indicate that the negative surface charge of quartz started decreasing with increasing DAH concentration, and after approximately 4×5.10^{-4} mol/L DAH concentration, the quartz particles acquired a positive charge, then the charge became +14.76 mV with the further increase in DAH concentration up to 1×10^{-3} mol/L.

As evident from the literature, since DAH is a weak electrolyte, the pH dictates its dissociation behavior [34]. Additionally, in the pH range of 6 to 7, and a DAH concentration lower than the critical micelle concentration (cmc) of DAH (1×5.10^{-2} mol/L), colloidal precipitation and micellization are not expected in the suspension. In this context, the adsorption of DAH molecules on quartz depends on the pH and the DAH concentration. Since the most dominant species in DAH solutions are monomeric alkyl ammonium (RNH_3^+) cations (see Figure 3b) at the natural pH of quartz suspension (pH 6.3), RNH_3^+ cations physically adsorb on the negatively charged quartz surfaces.

Considering the zeta potential of quartz as −30.30 mV at its natural pH value, the surface charge of quartz becomes less negative (−24.92 mV) at 5×10^{-5} mol/L DAH. Thus, it was observed that the surface charge of quartz approached positivity with increasing DAH concentration. It is interesting to note that the surface charge of particles in collector suspensions is quite important in interpreting micro-flotation experiments and bubble–particle attachment measurements. A brief literature survey indicates that not only the

surface charge of particles but also that of bubbles are instrumental in governing the fruitful bubble–particle interactions leading to flotation recoveries [35]. In the literature [36], the presence of a polyoxyethylene methyl ether frother was found to lead to a decrease in induction time values when the bubbles and the particles carried opposite charges, which in turn significantly changed the flotation recoveries. This point of view emphasizes the measurement of the electrical charge of bubbles to better explain the relation between attachment time and flotation recoveries, which would be carried out in future studies.

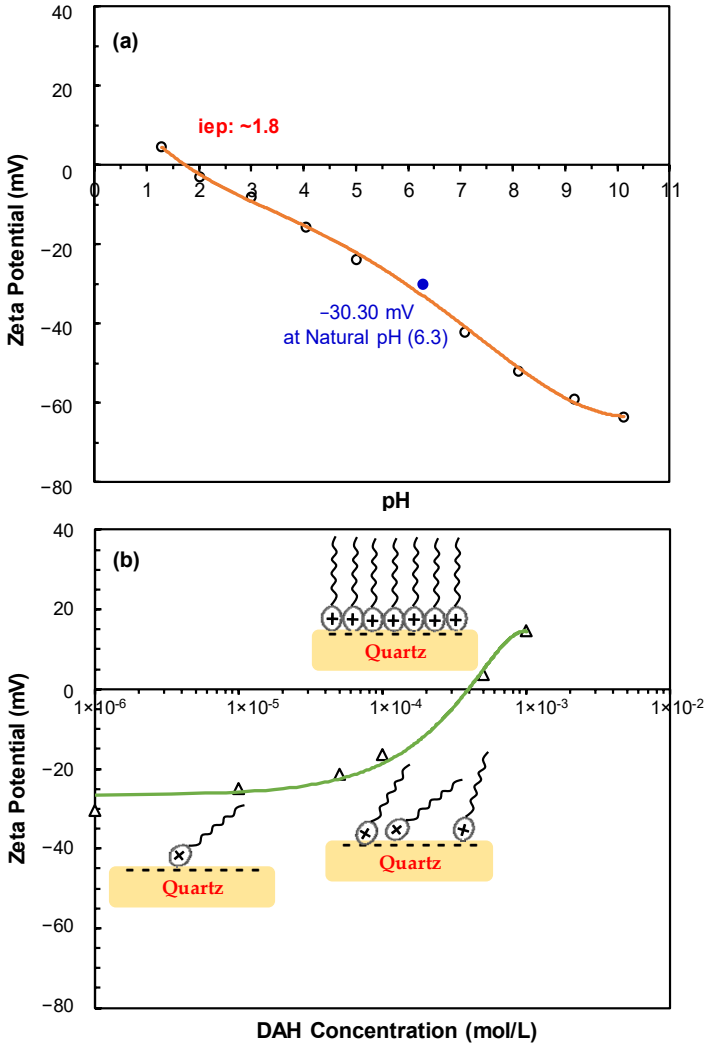

Figure 3. (**a**) Zeta potential pH profile of quartz in the absence of DAH; (**b**) Zeta potential of quartz as a function of DAH concentration at natural pH (between 6.25 and 5.71 from 1×10^{-5} mol/L DAH to 1×10^{-3} mol/L DAH).

3.2. Bubble–Particle Attachment Measurements

The results of the bubble–particle attachment measurements are more representative than contact angle measurements in comparing the hydrophobicity of particles, hence the flotation response of the minerals under defined conditions. For this reason, a series of bubble–particle attachment measurements were carried out with quartz particles of −38 + 20 µm in size to determine the effect of DAH concentration on the bubble–particle interactions. The variations in contact time with bubble particle attachment efficiency as well as bubble–particle attachment time at different DAH collector concentrations using a 0.5 mm capillary tube are shown in Figure 4.

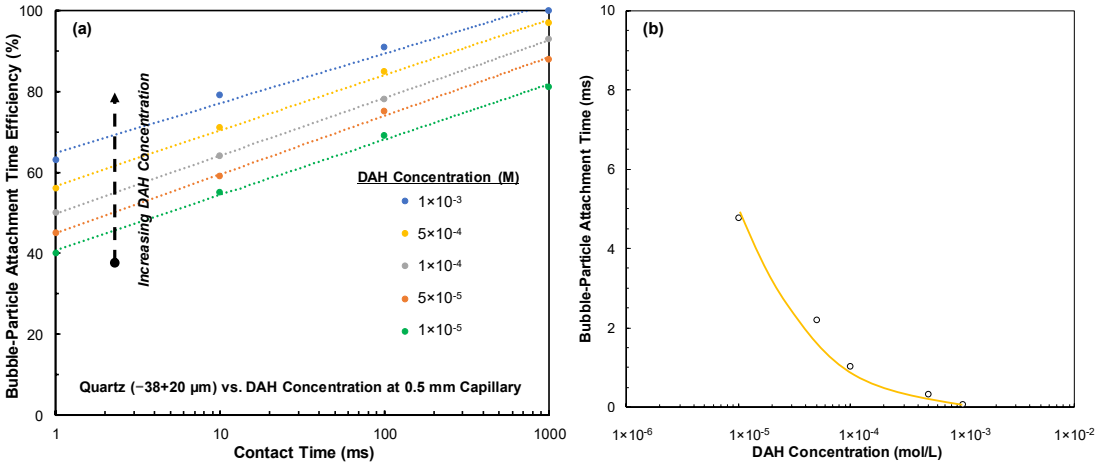

Figure 4. (**a**) Bubble–particle attachment time efficiency of −38 + 20 µm quartz particle vs. contact time; (**b**) Bubble–particle attachment time as a function of DAH concentration.

As seen in Figure 4a, the bubble–particle attachment efficiency of the quartz particles increased with the increasing contact time at all DAH concentrations. In other words, the bubble particle attachment efficiency for particles −38 + 20 µm in size was found to be approximately 55% at 1×10^{-5} mol/L DAH concentration at 10 ms contact time and increased to around 79% at 1×10^{-3} mol/L DAH concentration. The results also showed that the attachment of particles became more stable upon increasing the collector concentration in the system. The images taken during the bubble–particle attachment measurements presented in Figure 5 also clearly support the bubble–particle attachment efficiencies. As seen in Figure 5, the amount of quartz particles attached to the bubble surface increased with increasing contact time and DAH concentration.

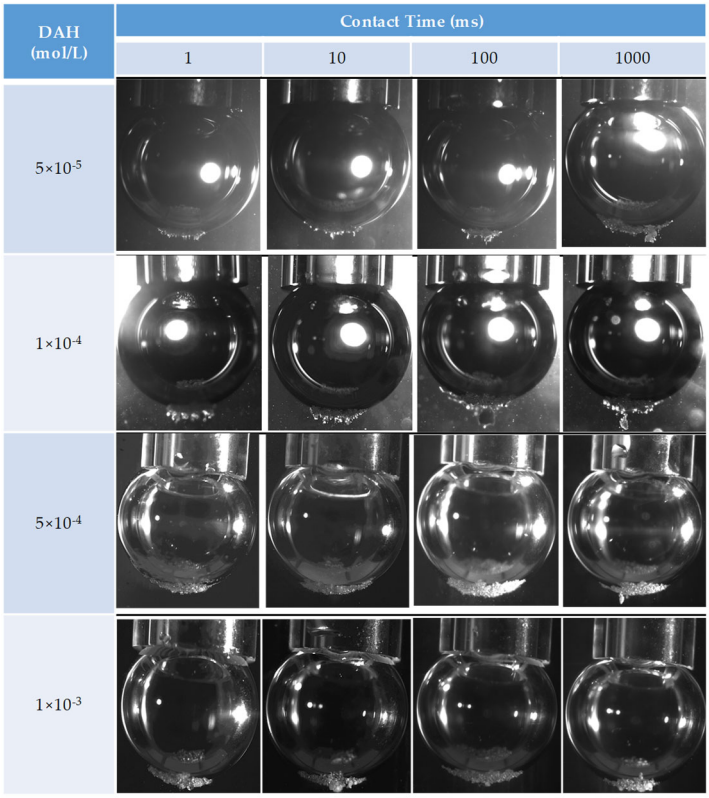

Figure 5. Pictures of bubble attachment to particles (−38 + 20 µm) at various DAH concentrations using a 0.5 mm capillary tube.

3.3. Micro-Flotation Experiments

A series of flotation experiments were conducted to find a correlation between flotation and bubble–particle interactions. The same collector concentrations were used with the previous experiments to determine the effect of different frothers on floatability at the same particle size range of −38 + 20 µm. Towards this aim, a series of micro-flotation experiments was conducted as a function of DAH concentration, and the results of these experiments are shown in Figure 6. As seen in Figure 6, in line with the expectation, a linear increase in flotation recovery was obtained as a function of DAH concentration.

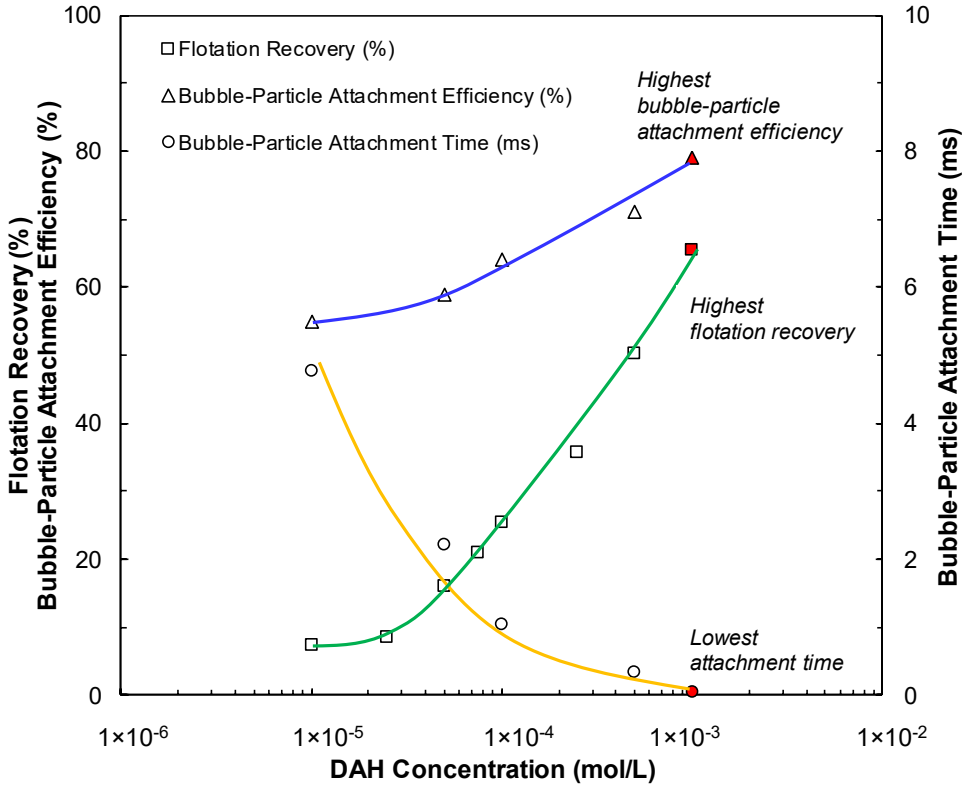

Figure 6. Results of % flotation recovery, % bubble–particle attachment efficiency at 10 ms contact time, and bubble–particle attachment time (ms) of quartz (−38 + 20 µm) particles as a function of DAH concentration.

Similar trends were also reported in the literature for the effect of amine concentration on the flotation recovery of quartz particles [37]. While the flotation recovery was around 40% for coarse particles in the size range of −297 + 150 µm, an almost linear increase was obtained until about 70% recovery upon decreasing the size to −74 + 38 µm at the same collector dosage of 20 g/t at a pH value adjusted to 9.0. However, as mentioned in a recent study, the recoveries may decrease in the case of pH values being kept around 7 regardless of DAH concentration in the system [38]. These results reveal that regardless of the hydrodynamic conditions during the flotation process, the flotation recovery of finer-sized quartz particles will be better. Our micro-flotation results as a function of collector concentration appear to be in line with these previous findings.

As also seen in Figure 6, while the bubble–particle attachment efficiency increased, conversely, the bubble–particle attachment time showed an apparent decrease with increasing DAH concentrations. It is interesting to note that the highest flotation recovery was obtained at the highest attachment efficiency; hence, the lowest bubble–particle attachment time indicated a strong relationship between the flotation recovery and the bubble–particle attachment time.

Meanwhile, since the collector DAH also functioned as a frother, its role during the micro-flotation experiments was studied as a function of frother type at their CCC values in the presence of DAH. Towards this aim, the concentration corresponding to 50% recovery (~5×10^{-4} mol/L) was selected as a reference concentration for future experiments to investigate the contribution of different frother types on flotation recoveries. The results of this series of experiments are shown in Figure 7. The results showed that the highest and lowest flotation recoveries were obtained with PPG600 and PPG200, respectively. According to the results shown in Figure 7, at high DAH concentrations and the CCC concentration of each respective frother, the flotation recoveries exhibited relatively low dependence indicative of the strong frothing ability of the DAH collector.

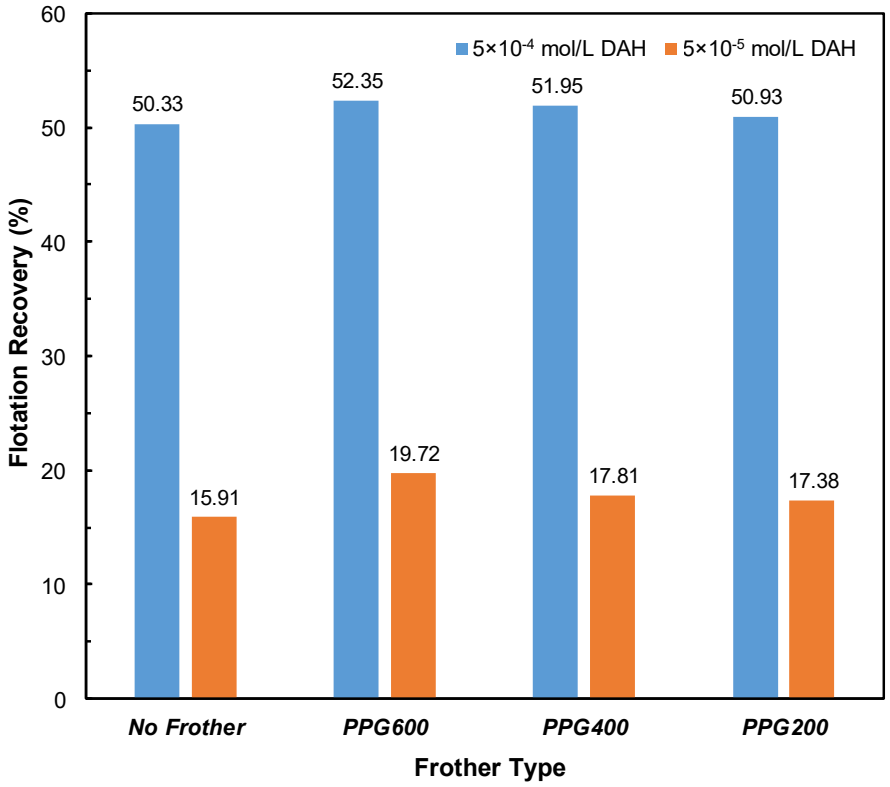

Figure 7. Flotation of quartz particle (−38 + 20 µm) at constant DAH concentration (5×10^{-4} mol/L) in the presence of different frothers (CCC concentrations).

With this information in mind, another set of experiments was performed at a lower DAH concentration (5×10^{-5} mol/L) to maximize the effect of the frother during the flotation experiments. As also shown in Figure 7, while a 15.91% recovery was achieved in the absence of frothers, an approximately 3% higher flotation recovery was obtained with the addition of PPG600 (3 ppm), indicating the higher dependency of the frother in this case. The overall results indicated that the frothing ability of DAH masked the performance of the frothers.

Considering these changes in flotation recoveries of fine-sized quartz particles and the higher contribution of PPG600 to its recovery, another set of experiments, especially as a function of PPG600 concentration at a constant DAH concentration (5×10^{-4} mol/L), was carried out. The results of these experiments shown in Figure 8 demonstrated that upon increasing the frother concentration in the suspension, relatively better-improved recoveries could be obtained as a function of frother concentration; apparently, there was a slight increase in the recovery values after the CCC value of PPG600 at 3 ppm. This can be attributed to the increased number of bubbles in the same volume, so higher amounts of particles can be carried into the foam as reported in our earlier study [39].

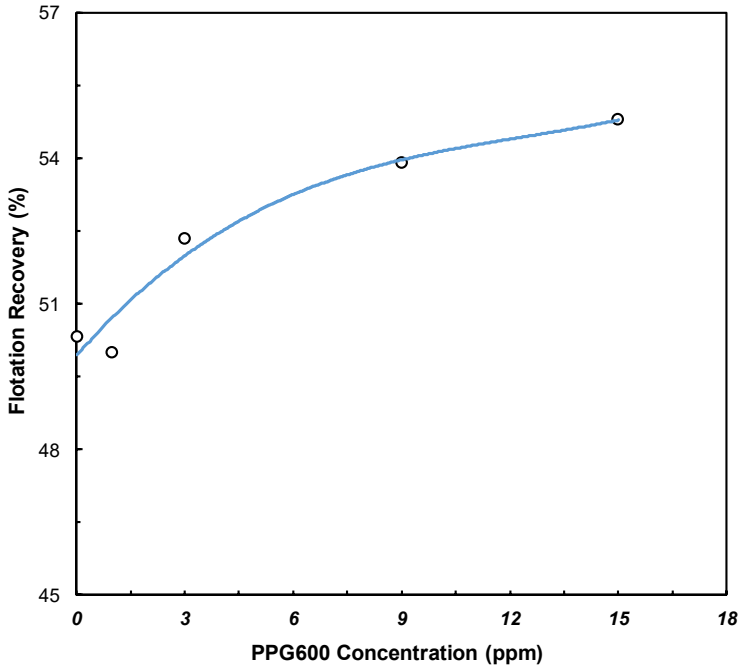

Figure 8. Flotation of quartz particles (−38 + 20 µm) at constant DAH concentration of 5×10^{-4} mol/L as a function of PPG600 concentration.

As known in the literature, long-chain alkyl or alkyl ether amines are widely used in quartz flotation as collectors, which can act as both a frother and a collector [40–43]. The results from the previous studies indicated that the foamability significantly varied with the frother type [15]. These results showed that while the highest foamability was obtained with PPG600 at its CCC value, the lowest foamability was found in the presence of PPG200. This can be easily attributed to the frothing feature of DAH in addition to its role as a collector in flotation [5]. It was reported that a significant decrease was also obtained in terms of the CCC for MIBC in the presence of 4 mg/L dodecylamine (DA). Our previous results showed that the use of DAH as a frother + collector mixture resulted in lowering the CCC values of frothers such as PPG600, 400, and 200 due to its additional frothing power during the flotation of particles [14].

From these results, it can be clearly understood that while the frothing ability of the collector in flotation dominates at higher concentrations, the frother becomes effective at lower collector concentrations. In addition, considering the use of different frothers of varying molecular weights, higher flotation recoveries could be obtained with the frother of the highest molecular weight within a homologous series.

As mentioned in the previous sections, the zeta potential and bubble–particle attachment efficiency and time characteristics of quartz at different DAH concentrations vividly showed that the quartz particles became more hydrophobic upon increasing the collector concentration. As is well-documented in the literature, the probability of the bubble attachment to solid surfaces depends on many factors, but mainly on the stability and drainage of the wetting film [44–46]. In addition, the effects of measurement parameters such as air bubble size, particle size, pH, and the mode of measurement like the polished surface or particle bed also have important implications on the results of measurements [30,47]. These results can be used as an indicator to explain our experimental results under different conditions. A previous study conducted by Albijanic et al. [48] reported a proportional decrease in the bubble–particle attachment efficiency at higher collector concentrations of sodium isobutyl xanthate (SIBX).

From this point of view, a series of flotation experiments was conducted to concurrently support these findings and the results suggest a strong correlation between flotation and bubble–particle interactions. Additionally, the flotation experiments were continued at

higher and lower DAH concentrations with the frothers at their CCC values to observe the possible positive or negative effects of DAH. The flotation results with frothers indicated that while the highest flotation recovery was obtained with PPG600 at its CCC values, the lowest flotation recovery was found in the presence of PPG200. The effect of PPG600 on the flotation system was more pronounced compared to the others for producing fine bubbles in the pulp zone compared to the performance of the other two frothers [15]. Additionally, the interaction between PPG600 and DAH led to a mutual synergistic effect, resulting in enhanced froth performance. This in turn resulted in finer bubble sizes, which affected the flotation recoveries of very fine particles [49–53].

4. Conclusions

In this study, the effect of several commercial frothers on the flotation recovery of the DAH/frother/quartz flotation system was investigated. The results for the zeta potential measurements of quartz particles in the absence and presence of DAH showed that the iep of quartz was determined at approximately pH 1.8. The surface charge of quartz particles with the addition of DAH to the suspension reversed its sign from negative to positive, indicating the physical adsorption of DAH on the quartz surfaces, as apparent from the literature.

The bubble–particle attachment time measurements showed that the bubble–particle attachment efficiency increased as a function of DAH concentration for the −38 + 20 µm particle size. Similarly, the micro-flotation experiments of quartz particles in the presence of DAH showed a linear dependence on the DAH concentration. The highest flotation recovery was obtained at the lowest bubble–particle attachment time, indicating a strong relationship between the flotation recovery and the bubble–particle attachment time.

Since hydrophilic minerals such as quartz may not require a frother, the collector alone can provide the required bubble size distribution above a certain DAH concentration. Because of this, the addition of different frothers to the quartz/DAH system produced relatively marginal changes in recoveries. While at the CCC concentration of each respective frother and a high DAH concentration (5×10^{-4} mol/L), the flotation recoveries exhibited a relatively low dependence, indicative of the strong frothing ability of the DAH collector; at a lower DAH concentration (5×10^{-5} mol/L), however, the addition of PPG600 at 3 ppm indicated a higher dependency of the frother. The overall results indicated that the strong frothing ability of DAH masked the performance of the frothers. Of course, the frothing performance of the frother + collector mixture is a complicated phenomenon and needs more future research to better understand the exact synergy between them.

Author Contributions: Conceptualization, O.O. and F.B.; methodology, K.B., O.G. and O.O.; validation, F.B. and Y.E.P.; investigation, K.B., O.G. and O.O.; resources, O.G., O.O., F.B. and M.S.Ç.; writing—original draft preparation, K.B., O.G. and O.O.; writing—review and editing, O.G., O.O., F.B. and M.S.Ç.; visualization, O.G., K.B. and Y.E.P.; supervision, O.G. and O.O.; project administration, M.S.Ç.; funding acquisition, M.S.Ç. All authors have read and agreed to the published version of the manuscript.

Funding: This project has received funding from the European Union's Horizon 2020 research and innovation program Fine Future under grant agreement No 821265.

Data Availability Statement: The original contributions presented in the study are included in the article.

Conflicts of Interest: The authors declare no conflict of interest.

References

1. Leja, J. *Surface Chemistry of Froth Flotation*; Plenum Press: New York, NY, USA, 1982.
2. Ahmed, N.; Jameson, G.J. The Effect of Bubble Size on the Rate of Flotation of Fine Particles. *Int. J. Miner. Process.* **1985**, *14*, 195–215. [CrossRef]
3. Yoon, R.H.; Luttrell, G.H. The Effect of Bubble Size on Fine Coal Flotation. *Coal Prep.* **1986**, *2*, 179–192. [CrossRef]
4. Tao, D. Role of Bubble Size in Flotation of Coarse and Fine Particles—A Review. *Sep. Sci. Technol.* **2005**, *39*, 741–760. [CrossRef]

5. Corona-Arroyo, M.A.; Lopez-Valdivieso, A.; Laskowski, J.S.; Encinas-Oropesa, A. Effects of Frothers and Dodecylamine on Bubble Size and Gas Holdup in a Downflow Column. *Miner. Eng.* **2015**, *81*, 109–115. [CrossRef]
6. Yoon, R.H.; Luttrell, G.H. The Effect of Bubble Size on Fine Particle Flotation. In *Frothing in Flotation*; Laskowski, J.S., Ed.; Gordon and Breach Science Publishers: Langhorne, PA, USA, 1989.
7. Cho, Y.S.; Laskowski, J.S. Effect of Flotation Frothers on Bubble Size and Foam Stability. *Int. J. Miner. Process.* **2002**, *64*, 69–80. [CrossRef]
8. Bournival, G.; Ata, S.; Karakashev, S.I.; Jameson, G.J. An investigation of Bubble Coalescence and Post-Rupture Oscillation in Non-ionic Surfactant Solutions Using High-Speed Cinematography. *J. Colloid Interface Sci.* **2014**, *414*, 50–58. [CrossRef]
9. Yoon, R.H. The Role of Hydrodynamic and Surface Forces in Bubble–Particle Interaction. *Int. J. Miner. Process.* **2000**, *58*, 129–143. [CrossRef]
10. Fan, X.; Zhang, Z.; Li, G.; Rowson, N.A. Attachment of Solid Particles to Air Bubbles in Surfactant-Free Aqueous Solutions. *Chem. Eng. Sci.* **2004**, *59*, 2639–2645. [CrossRef]
11. Nguyen, A.V.; Schulze, H.J. *Colloidal Science of Flotation*; Marcel Dekker: New York, NY, USA, 2004.
12. Woodburn, E.T.; Flynn, S.A.; Cressey, B.A.; Cressey, G. The Effect of Froth Stability on The Beneficiation of Low-Rank Coal by Flotation. *Powder Technol.* **1984**, *40*, 167–177. [CrossRef]
13. Subrahmanyam, T.V.; Forssberg, E. Froth Stability Particle Entrainment and Drainage in Flotation. *Int. J. Miner. Process.* **1988**, *23*, 33–53. [CrossRef]
14. Batjargal, K.; Guven, O.; Ozdemir, O.; Karakashev, S.; Grozev, N.A.; Boylu, F.; Çelik, M.S. Bubbling Properties of Frothers and Collectors Mix System. *Physicochem. Probl. Miner. Process.* **2022**, *58*, 152890. [CrossRef]
15. Batjargal, K.; Guven, O.; Ozdemir, O.; Karakashev, S.I.; Grozev, N.A.; Boylu, F.; Çelik, M.S. Frothing Performance of Frother-Collector Mixtures as Determined by Dynamic Foam Analyzer and Its Implications in Flotation. *Minerals* **2023**, *13*, 242. [CrossRef]
16. Fosu, S.; Skinner, W.; Zanin, M. Detachment of Coarse Composite Sphalerite Particles from Bubbles in Flotation: Influence of Xanthate Collector Type and Concentration. *Miner. Eng.* **2015**, *71*, 73–84. [CrossRef]
17. Ulusoy, U.; Yekeler, M.; Hiçyilmaz, C. Determination of the Shape, Morphological and Wettability Properties of Quartz and Their Correlations. *Miner. Eng.* **2003**, *16*, 951–964. [CrossRef]
18. Koh, P.T.L.; Hao, F.P.; Smith, L.K.; Chau, T.T.; Bruckard, W.J. The Effect of Particle Shape and Hydrophobicity in Flotation. *Int. J. Miner. Process.* **2009**, *93*, 128–134. [CrossRef]
19. Little, L.; Mainza, A.N.; Becker, M.; Wiese, J.G. Using Mineralogical and Particle Shape Analysis to Investigate Enhanced Mineral Liberation through Phase Boundary Fracture. *Powder Technol.* **2016**, *301*, 794–804. [CrossRef]
20. Xia, W.; Yang, J.; Zhu, B. Flotation of Oxidized Coal Dry-Ground with Collector. *Powder Technol.* **2012**, *228*, 324–326. [CrossRef]
21. Hewitt, D.; Fornasiero, D.; Ralston, J. Bubble Particle Attachment Efficiency. *Miner. Eng.* **1994**, *7*, 657–665. [CrossRef]
22. Verrelli, D.I.; Albijanic, B. A Comparison of Methods for Measuring the Induction Time for Bubble-Particle Attachment. *Miner. Eng.* **2015**, *80*, 8–13. [CrossRef]
23. Cao, Q.; Cheng, J.; Wen, S.; Li, C.; Bai, S.; Liu, D. A Mixed Collector System for Phosphate Flotation. *Miner. Eng.* **2015**, *78*, 114–121. [CrossRef]
24. Fuerstenau, D.W. Pradip. Zeta Potentials in the Flotation of Oxide and Silicate Minerals. *Adv. Colloid Interface Sci.* **2005**, *114–115*, 9–26. [CrossRef] [PubMed]
25. Ignatkina, V.A.; Bocharov, V.A.; Aksenova, D.D.; Kayumov, A.A. Zeta Potential of the Surface of Ultrafine Sulfides and Floatability of Minerals. *Russ. J. Non-Ferr. Met.* **2017**, *58*, 95–100. [CrossRef]
26. Albijanic, B.; Nimal Subasinghe, G.K.; Bradshaw, D.J.; Nguyen, A.V. Influence of Liberation on Bubble-Particle Attachment Time in Flotation. *Miner. Eng.* **2015**, *74*, 156–162. [CrossRef]
27. Melo, F.; Laskowski, J.S. Fundamental Properties of Flotation Frothers and Their Effect on Flotation. *Miner. Eng.* **2006**, *19*, 766–773. [CrossRef]
28. Guven, O.; Batjargal, K.; Ozdemir, O.; Karakashev, S.I.; Grozev, N.A.; Boylu, F.; Çelik, M.S. Experimental Procedure for the Determination of the Critical Coalescence Concentration (CCC) of Simple Frothers. *Minerals* **2020**, *10*, 617. [CrossRef]
29. Ulusoy, U. Dynamic Image Analysis of Differently Milled Talc Particles and Comparison by Various Methods. *Part. Sci. Technol.* **2018**, *36*, 332–339. [CrossRef]
30. Ye, Y.; Khandrika, S.M.; Miller, J.D. Induction-Time Measurements at a Particle Bed. *Int. J.* **1989**, *25*, 221–240. [CrossRef]
31. Albijanic, B.; Ozdemir, O.; Nguyen, A.V.; Bradshaw, D. A Review of Induction and Attachment Times of Wetting Thin Films Between Air Bubbles and Particles and its Relevance in Flotation Separation of Particles. *Adv. Colloid Interface Sci.* **2010**, *159*, 1–21. [CrossRef]
32. Karakashev, S.I.; Grozev, N.A.; Mircheva, K.; Ata, S.; Bournival, G.; Hristova, S.; Ozdemir, O. Surface Chemistry Tuning Solutions for Flotation of Fine Particles. *Minerals* **2023**, *13*, 957. [CrossRef]
33. Zhou, C.; Liu, L.; Chen, J.; Min, F.; Lu, F. Study on the Influence of Particle Size on the Flotation Separation of Kaolinite and Quartz. *Powder Technol.* **2022**, *408*, 117747. [CrossRef]
34. Laskowski, J.S.; Vurdela, R.M.; Liu, Q. The Colloid Chemistry of Weak Electrolyte–Collector Flotation. In Proceedings of the 16th International of Mineral Processing Congress, Stockholm, Sweden, 5–10 June 1988; pp. 703–715.
35. Yoon, R.H.; Yordan, J.L. Induction Time Measurements for the Quartz-Amine Flotation System. *J. Colloid Interface Sci.* **1991**, *141*, 374–383. [CrossRef]

36. Yoon, R.H.; Yordan, J.L. Zeta-Potential Measurements on Microbubbles Generated Using Various Surfactants. *J. Colloid Interface Sci.* **1986**, *113*, 430–438. [CrossRef]
37. Vieira, A.M.; Peres, A.E.C. The Effect of Amine Type, pH, and Size Range in the Flotation of Quartz. *Miner. Eng.* **2007**, *20*, 1008–1013. [CrossRef]
38. Zhou, J.; Chen, Y.; Li, W.; Song, Y.; Xu, W.; Li, K.; Zhang, Y. Mechanism of Modified Ether Amine Agents in Petalite and Quartz Flotation Systems under Weak Alkaline Conditions. *Minerals* **2023**, *13*, 825. [CrossRef]
39. Batjargal, K.; Guven, O.; Ozdemir, O.; Karakashev, S.I.; Grozev, N.A.; Boylu, F.; Çelik, M.S. Adsorption Kinetics of Various Frothers on Rising Bubbles of Different Sizes under Flotation Conditions. *Minerals* **2021**, *11*, 304. [CrossRef]
40. Smith, R.W.; Scott, J.L. Mechanisms of Dodecylamine Flotation of Quartz. *Miner. Process. Extr. Met. Rev.* **1990**, *7*, 81–94. [CrossRef]
41. Kowalczuk, P.B. Flotation and Hydrophobicity of Quartz in the Presence of Hexylamine. *Int. J. Miner. Process.* **2015**, *140*, 66–71. [CrossRef]
42. Bu, X.; Evans, G.; Xie, G.; Peng, Y.; Zhang, Z.; Ni, C.; Ge, L. Removal of Fine Quartz from Coal-Series Kaolin by Flotation. *Appl. Clay Sci.* **2017**, *143*, 437–444. [CrossRef]
43. Ren, L.; Qiu, H.; Zhang, Y.; Nguyen, A.V.; Zhang, M.; Wei, P.; Long, Q. Effects of Alkyl Ether Amine and Calcium Ions on Fine Quartz Flotation and its Guidance for Upgrading Vanadium from Stone Coal. *Powder Technol.* **2018**, *338*, 180–189. [CrossRef]
44. Verwey, E.J.W.; Overbeek, J.T.G. *Theory of the Stability of Lyophobic Colloids*; Elsevier: Amsterdam, The Netherlands, 1948; p. 218.
45. Ivanov, I.B.E. *Thin Liquid Films*; Marcel Dekker: New York, NY, USA, 1988.
46. Zawala, J.; Kosior, D. Dynamics of Dewetting and Bubble Attachment to Rough Hydrophobic Surfaces—Measurements and Modelling. *Miner. Eng.* **2016**, *85*, 112–122. [CrossRef]
47. Wang, X.; Miller, J.D. Dodecyl Amine Adsorption at Different Interfaces During Bubble Attachment/Detachment at A Silica Surface. *Physicochem. Probl. Miner. Process.* **2018**, *54*, 81–88.
48. Albijanic, B.; Bradshaw, D.J.; Nguyen, A.V. The Relationships between the Bubble-Particle Attachment Time, Collector Dosage and the Mineralogy of a Copper Sulfide Ore. *Miner. Eng.* **2012**, *36–38*, 309–313. [CrossRef]
49. Derjaguin, B.V.; Dukhin, S.S.; Rulyov, N.N. Kinetic Theory of Flotation of Small Particles. In *Surface and Colloid Science*; Matijević, E., Good, R.J., Eds.; Springer: Boston, MA, USA, 1984.
50. Karakashev, S.I.; Grozev, N.A.; Ozdemir, O.; Guven, O.; Ata, S.; Bournival, G.; Batjargal, K.; Boylu, F.; Hristova, S.; Çelik, M.S. Physical Restrictions of the Flotation of Fine Particles and Ways to Overcome Them. *Physicochem. Probl. Miner. Process.* **2022**, *58*, 153944. [CrossRef]
51. Farrokhpay, S.; Filippova, I.; Filippov, L.; Picarra, A.; Rulyov, N.; Fornasiero, D. Flotation of Fine Particles in the Presence of Combined Microbubbles and Conventional Bubbles. *Miner. Eng.* **2020**, *155*, 106439. [CrossRef]
52. Shahbazi, B.; Rezai, B.; Javad Koleini, S.M. Bubble-particle Collision and Attachment Probability on Fine Particles Flotation. *Chem. Eng. Process. Process Intensif.* **2010**, *49*, 622–627. [CrossRef]
53. Abrahamson, J. Collision Rates of Small Particles in a Vigorously Turbulent Fluid. *Chem. Eng. Sci.* **1975**, *30*, 1371–1379. [CrossRef]